SEMARAK ILMU PUBLISHING

Journal of Advanced Research in Micro and Nano Engineering

Journal homepage:
https://semarakilmu.com.my/journals/index.php/micro_nano_engineering/index
ISSN: 2756-8210

Characterization $BaFe_{12-3x}Co_xCu_xZn_xO_{19}$ Samples Based on Natural Iron Sand on Electrical and Magnetic Properties as a Microwave Absorbent Material

Susilawati[1,*], Aris Doyan[1], Ali M.A. Abdul Amir Al-Mokaram[2], Mohammed Ahmed Ali Omer[3], Muhammad Taufik[1], Saprizal Hadisaputra[4], Yana Taryana[5], Nanang Sudrajat[6], Dedi Riyan Rizaldi[7], Ziadatul Fatimah[8], Muhammad Ikhsan[9], Nuraini Rachma Ardianti[9]

[1] Physics Education, FKIP, University of Mataram, Jl. Majapahit No. 62 Mataram 83125, Indonesia
[2] Department of Chemistry, College of Science, Mustansiriyah University, Baghdad, 10052, Iraq
[3] Department of Radiologic Technology, College of Applied Medical Sciences, Qassim University, Buraidah, Saudi Arabia
[4] Chemistry Education, FKIP, University of Mataram, Jl. Majapahit No. 62 Mataram 83125, Indonesia
[5] Research Center for Telecommunication, National Research and Innovation Agency, Bandung, Indonesia
[6] Research Center for Electronics, National Research and Innovation Agency, Bandung, Indonesia
[7] MA Plus Nurul Islam Sekarbela, Mataram, Indonesia
[8] SMA NW Mataram, Mataram, Indonesia
[9] Balai Publikasi Indonesia, Mataram, Indonesia

ARTICLE INFO

Article history:
Received 11 September 2024
Received in revised form 17 October 2024
Accepted 20 November 2024
Available online 31 December 2024

Keywords:
$BaFe_{12-3x}Co_xCu_xZn_xO_{19}$; coprecipitation; microwave absorbing material; natural iron sand

ABSTRACT

Indonesia is one of the countries that has very large natural resources, one of which is related to iron sand. Iron sand is a type of sand with a significant concentration of iron. This is usually characterized by dark gray or blackish color conditions. The purpose of this study was to determine the characteristics of the synthesis results of BaFe12-3xCoxCuxZnxO19 from natural iron sand. The natural iron sand obtained was synthesized using the cooperativity method because its advantages are that it has a variety of conditions that can be selected starting from the ratio, temperature, pH, precipitating agent, and so on. In accordance with the desired final result, namely to create a soft magnetic powder so that it can be used as a basic material for microwave absorption with a high conductivity level of nanoparticle size. Economical basic materials can be used as an alternative in making samples. The results of the synthesis that have been carried out have succeeded in obtaining dark colored powder according to the variations in concentration and temperature carried out, and then the results of the characterization test were carried out to determine the absorption produced with the Vector Network Analyzer (VNA) tool, where the results obtained were quite high, namely 99.31%. This is because the sample is included in the semiconductor material, which is characterized by the conductivity value obtained ranging from 10-3 S/cm to 10-1 S/cm. According to the indicators, the sample has met the criteria to be applied as a microwave absorber material, namely having a nanoparticle size, being soft magnetic, and already being included in the semiconductor material.

* *Corresponding author.*
E-mail address: susilawatihambali@unram.ac.id

https://doi.org/10.37934/armne.28.1.8094

1. Introduction

In the last few decades, pollution in the form of electromagnetic interference has become a concern. This is in line with the rapid development of electronic technology and high-frequency telecommunication systems in the order of gigahertz (GHz). Electromagnetic pollution causes interference to the input systems of electronic devices [1], radar disturbance, reduces device performance, obfuscates even the malfunction of the device [2], and many others. Those disturbances cause prohibitive use of electronic devices such as mobile phones or smart phones in airplanes, gas stations, and in some vital places with electronic operating systems. To overcome this problem, a damping system that can absorb electromagnetic waves is needed [3,4].

Ferrite based materials, such as hexaferrite [5-9] and spinel ferrites [10-13], are extensively researched for application as absorber of electromagnetic waves. Hexaferrites are classified into several types depending on the crystal structure, namely M, W, Y, X, U, and Z [5]. The M type one of which is barium hexaferrite ($BaFe_{12}O_{19}$) [14], that has been widely explored for various applications due to several advantages of excellent chemical properties, resistance to corrosion, high magnetic coercivity and saturation, and high Curie temperatures [15,16], good cohesiveness [17] and large magneto crystalline anisotropy constant [18]. Due to its magnetic properties, it has also been explored as base material for absorbing electromagnetic waves [6,8]. After modification, it is then used as a coating for antiradar materials, such as aircraft and antiradar drones [19]. Previous studies reported that the barium hexaferrite material can be applied to several electronic devices [20,21], such as in the speaker [22], magnetic recording medium [7], and its potentially as tape recording and large data storage [21].

To be applicable for a good microwave absorber, further developments of ferrite materials are required [23]. The coercivity field of barium hexaferrite is still relatively high, so it is still not suitable for direct application as a microwave absorber [8]. The crystal structure and magnetic properties of barium hexaferrite based material need to be modified, for example, by doping (substitution) of Ba^{2+} or Fe^{3+} cations or with other transition metal cations, such as Zn, Al, Mg, Ga, Co, Mo, Ti, and Ni are taken from previous study [24-28]. Previous studies reported that ferrite-based materials with Fe substitution using Ni and Zn had been successfully synthesized, but the resulting coercivity field (Hc) was still too high [29]. The high coercivity field increased the anisotropic properties, which weakens its microwave absorption properties. Better results were shown when doping with Mg and Al, where magnetic saturation and remanence increased [8], while coercivity decreased to 2.3 kOe [27]. Multivalent metals such as $Ni^{2+/3+}$ and $Co^{2+/3+}$ for $Fe^{2+/3+}$ are frequently used due to their similarity in ionic radiation and electronic configurations [30]. Previous research claims that Co, Cu, and Zn are some of the best dopant materials for barium hexaferrite [31]. The resulting material is of interest for many applications [32], especially as a microwave absorber [33].

Based on this background, researchers are interested in conducting research aimed at developing barium M-hexaferrite-based materials that have the potential to be applied for microwave absorption. Material for such application is characterized by certain conductivity and magnetic properties. In this study, we developed barium M-hexaferrite-based materials by substituting the Fe element with Co, Cu, and Zn. The Co-Cu-Zn doping was hypothesized to alter static magnetic properties (especially reducing the coercivity and increasing saturation magnetization) at the critical substitution ratio, resulting in a new material more desirable for microwave absorption. The coercivity field of the material was expected to be reduced by making the powder size reach nano order, and the dopant ion was attempted to be similar in size to the substituted ion. The use of three metal ions as doping with different natural iron sands is expected to provide a significant effect

compared to previous research that has been done using only one or two dopings. The addition of doping is to prove the strength of electricity, absorption, and even the desired magnetic properties.

2. Methodology

2.1 Synthesis of $BaFe_{12-3x}Co_xCu_xZn_xO_{19}$

Modified barium M-hexaferrite ($BaFe_{12}O_{19}$) with Cobalt-Cupper-Zink dopant with concentrations (x = 0; 0.4; 0.8; and 1.0) was synthesized using the coprecipitation method. Natural iron sand, barium carbonate ($BaCO_3$, Merck), cobalt chloride ($CoCl_2$, Merck), copper (II) sulphate ($CuSO_4$), and $Zn(NO_3)_2$ were used as raw materials. $BaCO_3$ was first dissolved in 30 ml of HCl (12 M, Merck) at 70 ℃ on a hot plate and stirred for 2 hours, then cooled to room temperature for 30 minutes. This mixture was then put into a beaker of $FeCl_3$, $CoCl_2$, $CuSO_4$, and $Zn(NO_3)_2$, followed by adding 50 ml of distilled water and stirred using a magnetic stirrer at a speed of 500 rpm until it formed a homogeneous solution (around 30 minutes). Next, this mixture was added drop by drop with the precipitating agent NH_4OH (6.5 M, Merck) with a burette to enhance the deposition. The sample was then cooled and washed with distilled water until a neutral pH was obtained. The precipitate is then filtered with filter paper. Next, the precipitated material was dried at 80 ℃ using an oven. The dry precipitate was then ground to obtain a brownish powder and sintered at varying temperatures of 200, 600, and 1000 ℃ for 4 hours. The procedures related to the sample preparation and manufacturing process can be seen in Figure 1.

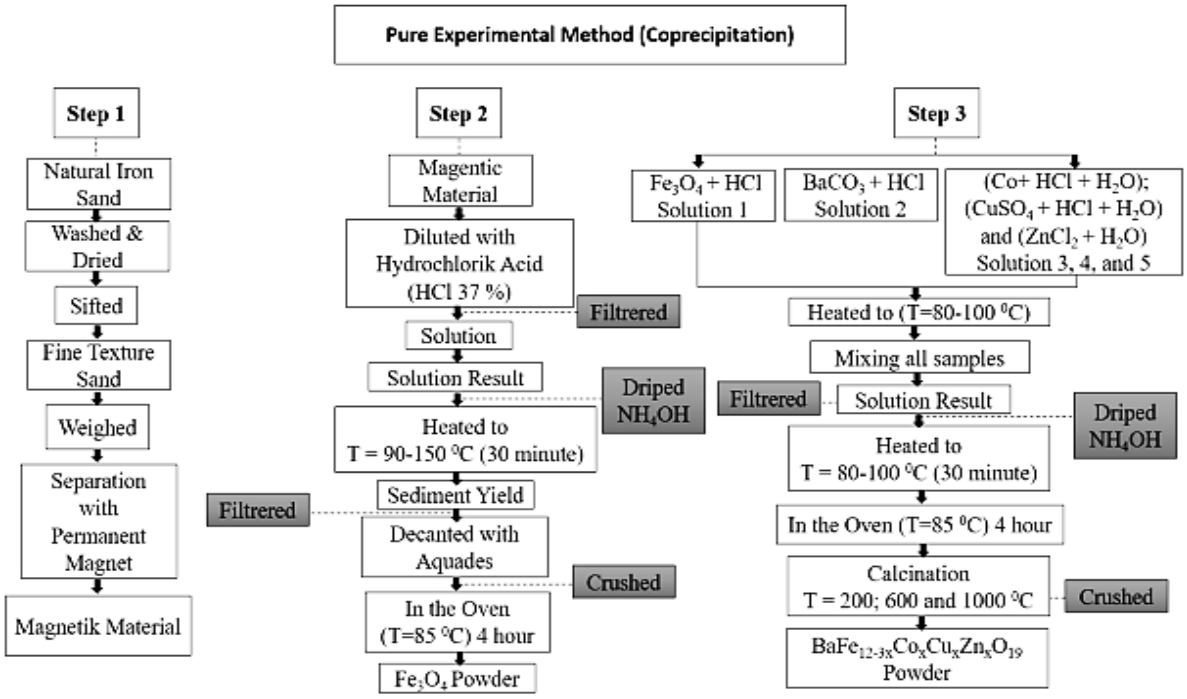

Fig. 1. Step 1 sample separation process, step 2 separation of Fe_3O_4 from magnetic materials, and step 3 synthesis process with coprecipitation method

2.2 Characterizations of $BaFe_{12-3x}Co_xCu_xZn_xO_{19}$

After the barium M-hexaferrite ($BaFe_{12-3x}O_{19}$) with Cobalt-Cupper-Zink dopants has been synthesized, it is then continued with the characterization process. The sample characterization tests used Fourier Transform Infra-Red (FT-IR), Transmission Electron Microscopy (TEM), Vibrating Sample

Magnetometer (VSM), and Vector Network Analyzer (VNA) as microwave-absorbing materials. The FTIR tool was used to determine the elements present in $BaFe_{12}O_{19}$ samples doped with Cobalt-Cupper-Zink with concentrations (x = 0; 0.4; 0.8; and 1.0) at temperatures (T = 1000 ℃). The TEM tool determines the particle size of the nanosized samples used in this research, namely concentration (x = 1.0) at temperature (T = 1000 ℃). The VSM tool is used to determine the magnetic properties of the material, and the VNA tool is used to find out how effectively the material can conduct electricity and how much absorption is produced by the sample as a microwave absorbing material, which is used in this research, namely concentration (x = 0; 0.4; 0.8; and 1.0) at temperatures (T = 200 ℃; 600 ℃; and 1000 ℃).

3. Results

3.1 Phase Identification

Fourier Transform Infra-Red (FT-IR) aims to describe the substitution process for the dopants used in the sample, namely cobalt (Co), copper (Cu), and zinc (Zn) on the crystal bond structure. The samples tested used the best temperature of 1000 ℃ with variations in concentration (mole fraction (x) = 0; 0.4; 0.8; and 1.0). The results of the analysis related to phase identification in the sample can be seen in Figure 2 and Table 1.

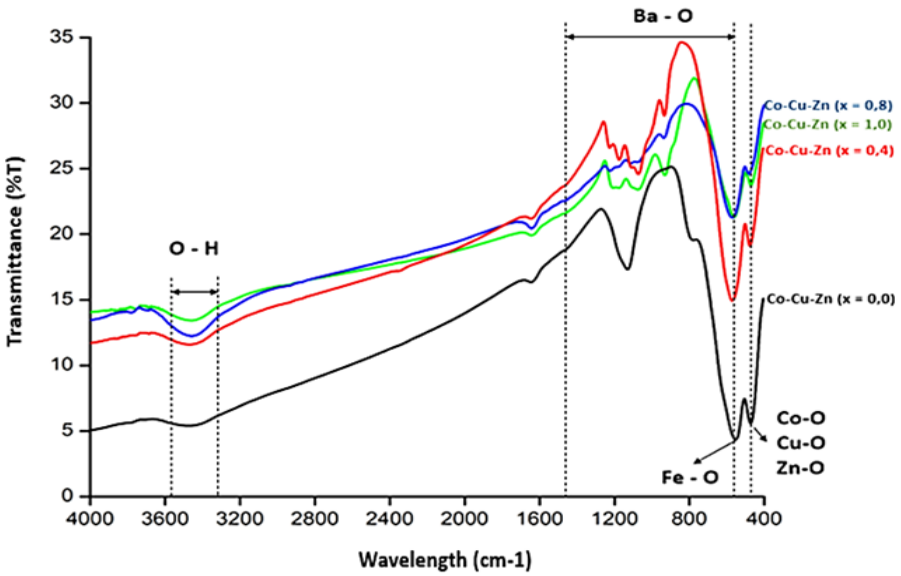

Fig. 2. Graph of the relationship between the percentage of transmittance (%T) with wave number (cm^{-1}) at x = 0.0; 0.4; 0.8; and 1.0 with T= 1000 ℃

The results of the FT-IR test above in the graph show the Ba-O metal bond at a peak of 1.124 cm^{-1}. The Ba-O wave number is in accordance with its characteristics, namely in the range of 1000 cm^{-1} to 1650 cm^{-1}. In addition to the Ba-O bond, another metal bond that is visible is Fe-O at a peak of 542 cm^{-1}. The wave number is in accordance with the range of Fe-O, which is in the range of 450 cm^{-1} to 690 cm^{-1}. Other bonds, namely Co-O, Cu-O, and Zn-O, are at a peak of 469 cm^{-1}. The wave number is in accordance with the range of the three bonds, namely in the range of 400 cm^{-1} to 663 cm^{-1}. The presence of wave bonds on the graph shows that the sample used is in accordance with the treatment, namely the presence of basic materials such as Ba and Fe that are doped with Co-Cu-Zn metal ions as binders or strengtheners in samples that are made to suit what is desired.

Table 1
Compound elements in the sample

Bonding type	The number of waves formed (cm^{-1})				Reference wave number (cm^{-1})	Reference sources
	x = 0	x = 0.4	x = 0.8	x = 1.0		
Ba-O	1075	1071	1078	1.130	895-1650	[34,35]
Fe-O	570	559	563	546	440-690	
Co-O	467	485	475	462	400-663	[36,37]
Cu-O	467	485	475	462		
Zn-O	467	485	475	462		

3.2 Morphology and Crystal Structure of $BaFe_{12-3x}Co_xCu_xZn_xO_{19}$

The size and structure of the powder particles can be identified using the Transmission Electron Microscope (TEM). The TEM results in Figure 3 show the crystal structure of $BaFe_{12}Co_{1.0}Cu_{1.0}Zn_{1.0}O_{19}$ sintered at a temperature of 1000 ℃. The TEM image clearly shows the size of the $BaFe_{12}Co_{1.0}Cu_{1.0}Zn_{1.0}O_{19}$ crystals formed. The test results showed that the crystal size obtained was 100 nm, still large enough to carry out further measurements, and a crystal size of 50 nm was obtained. Data related to the size of the crystal structure can be seen in Figure 3. More precisely, the information is in the lower right position of the image. This indicates that the sample we made is a nanoparticle. Nanoparticles are particles between 1 and 100 nanometers in size [38-40]. Larger dopant concentrations lead to larger crystal sizes [41,42]. Typically, smaller grain sizes (nano order) result in higher active energies that influence magnetic saturation and field coercivity [15,43,44].

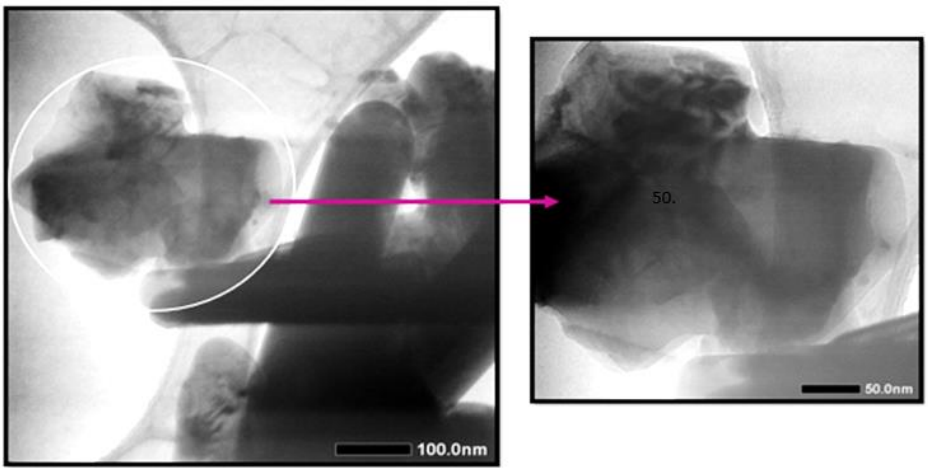

(a) (b)

Fig. 3. TEM test results on sample $BaFe_{12}Co_{1.0}Cu_{1.0}Zn_{1.0}O_{19}$ with T= 1000 ℃ (a) Crystal size 100 nm (b) Crystal size 50 nm

Based on the image in Figure 3, it can be seen that there are components formed, namely hexagonal, which is found in Figure 3, with a size of 50 nm, and when compared to previous researchers who only got a size of 100 nm, it can be said that the BaM sample with Co, Cu, and Zn metal ion doping managed to get a smaller size [45]. The results of this study are supported by the results of research conducted by Braun *et al.,* [46] and Oktavia and Sutoyo [47], which stated that the particle size of the sample can be expressed as nanoparticles because in each study they obtained a sample size of 100 nm to 20 nm. Nano-sized BaM samples have wide application opportunities [48,49]. One of its uses is in the electronics industry, namely as a microwave absorber [50,51].

3.3 Magnetic Properties and Conductivity of $BaFe_{12-3x}Co_xCu_xZn_xO_{19}$

The magnetic properties of a sample can be determined using a Vibrating Sample Magnetometer (VSM), where the values obtained in this test are saturation magnetization (Ms), remanence magnetization (Mr) and coercivity (Hc) [52,53]. The data on magnetic properties can be seen in Table 2.

Table 2
Magnetic properties of sample

T (℃)	Sample	Ms (emu/g)	Mr (emu/g)	Hc (T)
200	$BaFe_{12}O_{19}$	1.23	1.22	0.4400
	$BaFe_{10.8}Co_{0.4}Cu_{0.4}Zn_{0.4}O_{19}$	1.93	1.86	0.3500
	$BaFe_{9.6}Co_{0.8}Cu_{0.8}Zn_{0.8}O_{19}$	2.11	1.87	0.2100
	$BaFe_{9}Co_{1.0}Cu_{1.0}Zn_{1.0}O_{19}$	3.41	2.31	0.0900
600	$BaFe_{12}O_{19}$	1.38	1.32	0.3600
	$BaFe_{10.8}Co_{0.4}Cu_{0.4}Zn_{0.4}O_{19}$	3.40	3.00	0.2800
	$BaFe_{9.6}Co_{0.8}Cu_{0.8}Zn_{0.8}O_{19}$	6.46	5.64	0.2100
	$BaFe_{9}Co_{1.0}Cu_{1.0}Zn_{1.0}O_{19}$	9.49	6.28	0.0800
1000	$BaFe_{12}O_{19}$	1.51	1.43	0.3000
	$BaFe_{10.8}Co_{0.4}Cu_{0.4}Zn_{0.4}O_{19}$	7.27	6.07	0.2100
	$BaFe_{9.6}Co_{0.8}Cu_{0.8}Zn_{0.8}O_{19}$	11.09	7.91	0.1000
	$BaFe_{9}Co_{1.0}Cu_{1.0}Zn_{1.0}O_{19}$	26.80	9.80	0.0045

The value of Hc is inversely proportional to the value of Ms and Mr, namely, when the values of Ms and Mr increase, the Hc value decreases, which is close to zero on the hysteresis curve graph. This is in accordance with the theory that the value of the coercivity field (Hc) is obtained from demagnetization with a certain value so that the magnetization is zero, while saturation magnetization is a condition obtained from an increase in the external field that occurs from the origin point so that saturation occurs [54,55]. The saturation is because it has experienced alignment caused by an external magnetic field. From the saturation state and the zero-coefficient field, there is no return of the curve to its original shape but a residual magnetic flux. The remaining flux is called remanent magnetization. In this condition, the magnetic moment does not return to its orientation before being given an external field, which causes the material to be partially magnetized [56,57].

The results of the data obtained not only look at the magnetic properties of the material but also show how much doping influence and calcination temperature are used so that the characteristics of the magnetic hysteresis curve that can be used to conclude data that the magnetic material is included in soft magnetic or hard magnetic [58,59].

It can be seen the shape of the hysteresis curve of each sample in Figure 4. From these results, it can be seen the difference between the hysteresis curves at temperatures (T = 200 ℃; 600 ℃; and 1000 ℃) with each mole fraction, namely an increase in the value of Mr and Ms which causes the value of Hc to decrease. It can be said that there has been a process of magnetization caused by an increase in the external field, resulting in saturation and demagnetization. Demagnetization is the external field that is removed.

Based on Figure 4, it can be seen that there is an effect of doping and calcination temperature in the synthesis process to determine the value of the magnetic properties, which can be seen on the hysteresis curve. The decrease in the value of Hc and the increase in the value of Ms and Mr occurred due to the high doping and calcination temperatures used. In addition to decreasing the value of Hc, crystal size can also affect the inhibition of movement. The larger the size of the resulting crystal, the

easier it is for the domain wall to move so that the external magnetic field resistance is getting smaller, which causes the Hc value to decrease to near zero.

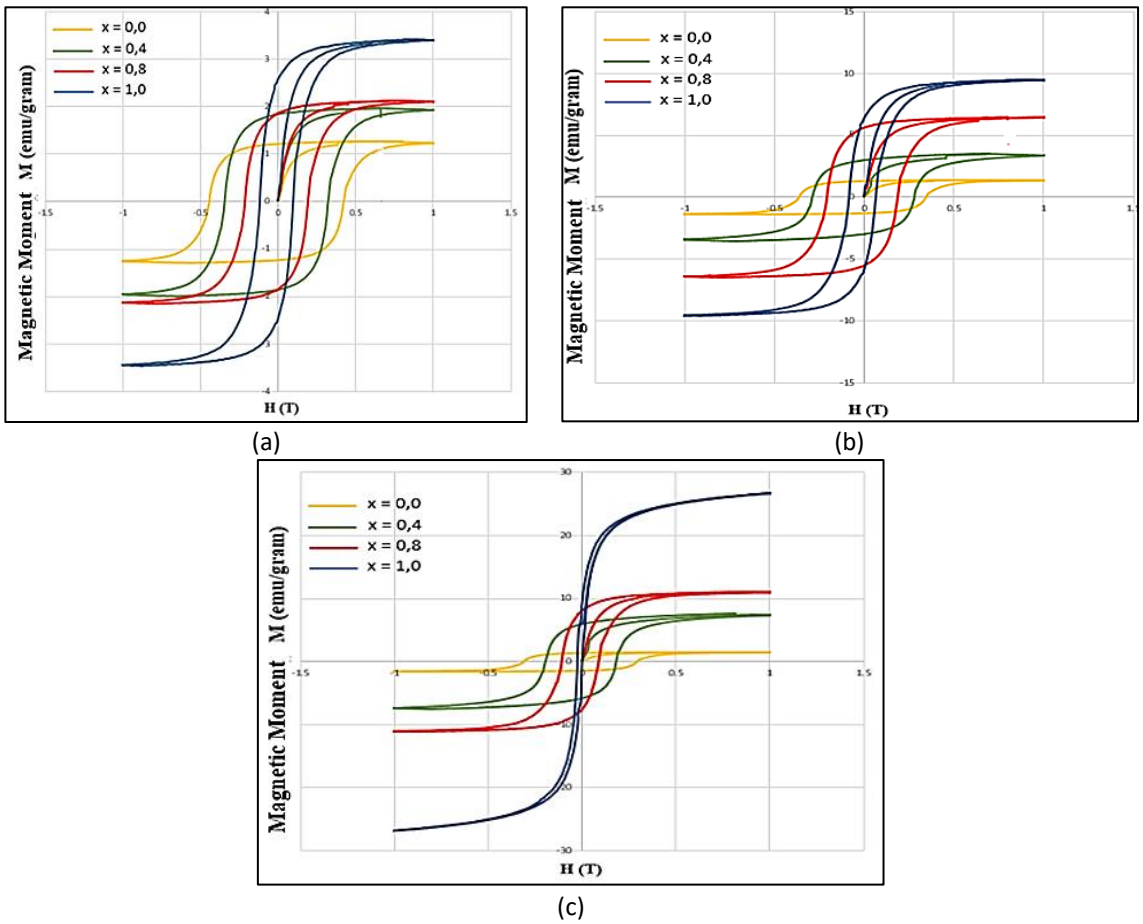

Fig. 4. Sample hysteresis curve (a) T= 200 ℃ (b) T= 600 ℃ (c) T= 1000 ℃

The magnetic properties of BaM in the $BaFe_9O_{19}$ sample show that the hysteresis curve becomes wider with large magnetization values (Ms and Mr) and coercivity field (Hc), which is different from the doped sample so that the magnetization increases (Ms and Mr) and decreases the coercivity field (Hc). Which makes the sample into a soft magnetic material. The results are indicated by the presence of a hysteresis curve when subjected to a magnetic field or when demagnetized, and can be seen from the width of the hysteresis curve, which is getting narrower. Which results in the material being soft and magnetic.

The electrical properties of the sample can be identified using a Vector Network Analyzer (VNA) tool. The data obtained starts at a frequency of 8-12 GHz, so the conductivity value of the sample is obtained using Eq. (1). The results of the analysis can be seen in Figure 5.

$$\sigma = \frac{l}{RA} \tag{1}$$

A good electrically conducting material has a conductivity of the order of 10^7 S/cm, whereas an insulator material has a very low conductivity between 10^{-10} S/cm and 10^{-20} S/cm. Between these two properties, semiconductor materials have a conductivity value of 10^{-7} to 10^3 S/cm [60,61]. Based on the results obtained, it can be concluded that the sample is very good for use as a microwave absorbent material because the semiconductor material can convert microwave energy into heat

energy. The formation of an electric field on the surface of the absorber occurs when the microwave hits the material coated with the microwave absorbent material, after which the current flows as a surface current so that it can convert microwaves into heat energy [62,63].

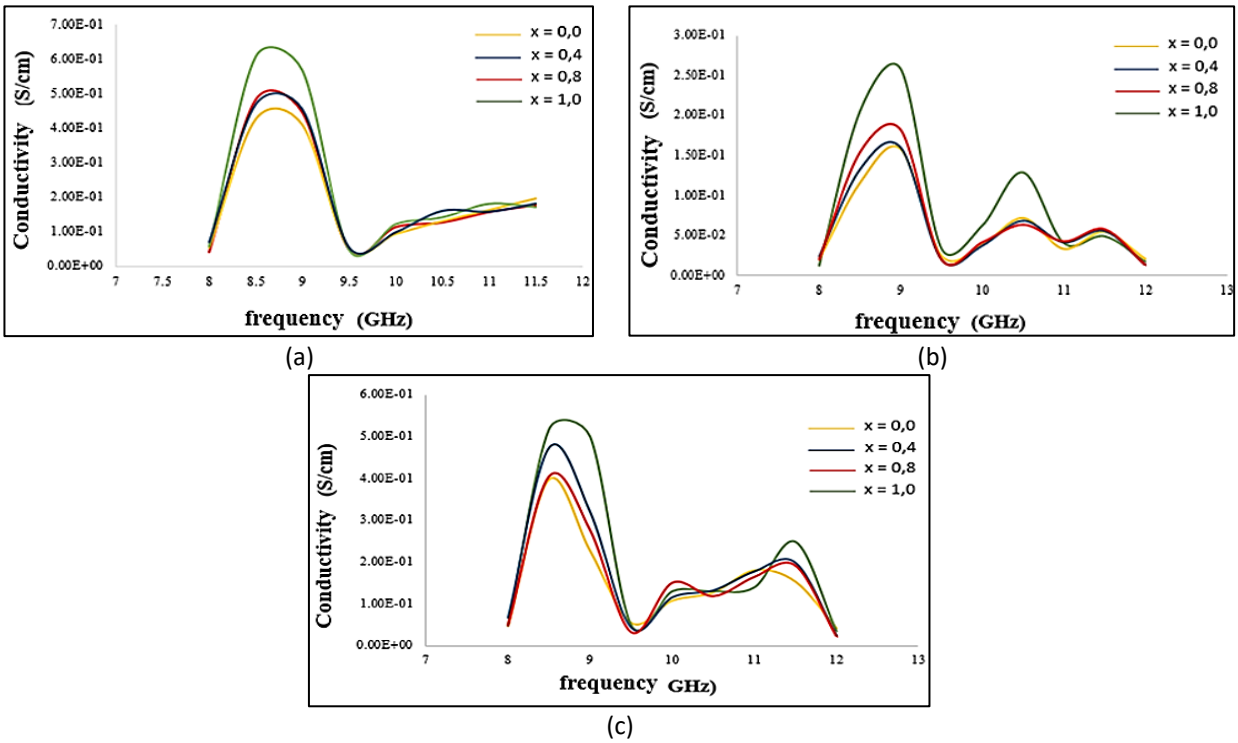

Fig. 5. Graph of the conductivity of the sample at x = 0.0, 0.4, 0.8, and 1.0 with (a) T= 200 ℃ (b) T= 600 ℃ (c) T= 1000 ℃

The relationship between the 8-12 GHz frequency and the Reflection Loss (dB), Reflection Coefficient (%) and Absorption (%) coefficient values has different values, and can be seen in Table 3, and Figures 6 to 8.

Table 3
Value of reflection loss (dB), reflection coefficient (%) and absorption (%)

T (℃)	Sample	F (GHz)	RL (dB)	RC (%)	A (%)
200	$BaFe_{12}O_{19}$	10.800	-7.897	16.229	83.770
	$BaFe_{10.8}Co_{0.4}Cu_{0.4}Zn_{0.4}O_{19}$	10.750	-8.018	15.783	84.216
	$BaFe_{9.6}Co_{0.8}Cu_{0.8}Zn_{0.8}O_{19}$	10.714	-9.642	10.859	89.140
	$BaFe_{9}Co_{1.0}Cu_{1.0}Zn_{1.0}O_{19}$	10.920	-11.771	6.651	93.449
600	$BaFe_{12}O_{19}$	10.710	-8.584	13.854	86.145
	$BaFe_{10.8}Co_{0.4}Cu_{0.4}Zn_{0.4}O_{19}$	10.680	-9.995	10.011	89.988
	$BaFe_{9.6}Co_{0.8}Cu_{0.8}Zn_{0.8}O_{19}$	11.060	-12.221	5.996	94.003
	$BaFe_{9}Co_{1.0}Cu_{1.0}Zn_{1.0}O_{19}$	10.750	-14.032	3.951	96.048
1000	$BaFe_{12}O_{19}$	11.200	-19.818	14.246	85.753
	$BaFe_{10.8}Co_{0.4}Cu_{0.4}Zn_{0.4}O_{19}$	11.060	-17.853	1.639	98.360
	$BaFe_{9.6}Co_{0.8}Cu_{0.8}Zn_{0.8}O_{19}$	10.800	-8.463	1.042	98.957
	$BaFe_{9}Co_{1.0}Cu_{1.0}Zn_{1.0}O_{19}$	10.680	-21.642	0.685	99.314

Figure 6 shows the relationship at a frequency of 8-12 GHz with the resulting Reflection Loss (dB) value where value of RL (dB) results at each frequency are different. The samples used were at a calcination temperature of 1000 ℃ with a concentration of x = 0.0 and 1.0. At a concentration of x = 0.0, the $BaFe_{12-3x}O_{19}$ sample had the highest RL (dB) value at a frequency of 10.68 GHz of -8.34 dB. At

the same frequency of 10.68 GHz, the concentration of x = 1.0 in the $BaFe_9Co_{1.0}Cu_{1.0}Zn_{1.0}O_{19}$ sample was 21.64 dB. The greater the negative value of the RL (dB), the greater the absorption results and the smaller the reflection. The RL value of the $BaFe_{12-3x}O_{19}$ sample of -8.34 dB has an absorption value of 85.69% and a reflection of 14.30%. For the $BaFe_9Co_{1,0}Cu_{1,0}Zn_{1,0}O_{19}$ sample, which has an RL value of -21.64 dB, it has an absorption value of 99.31% and a reflection of 0.68%. When compared with previous research conducted by Hambali and Doyan [61], the RL value obtained was -20.20 dB using Co-Mn-Ni metal doping. The greater the RL value (dB) produced, the higher the absorption percentage.

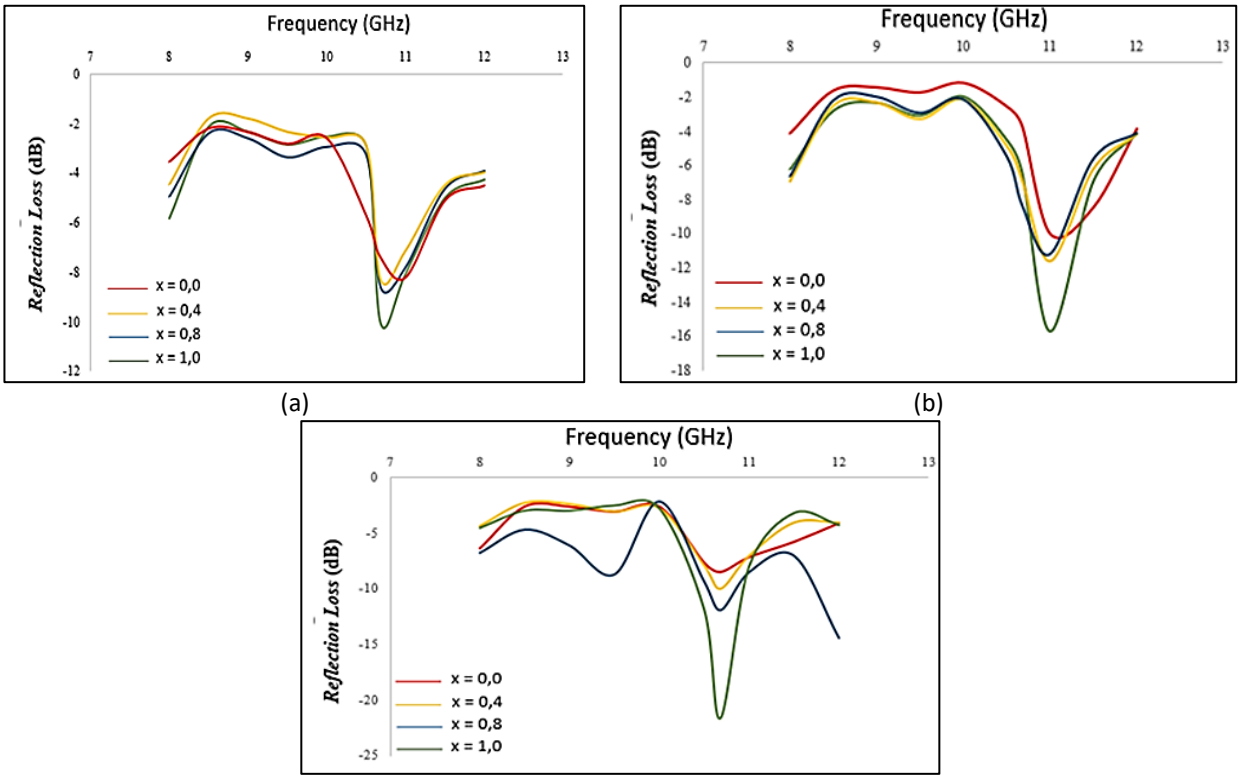

Fig. 6. Value chart RL (dB) at x = 0.0, 0.4, 0.8, and 1.0 with (a) T= 200 ℃ (b) T= 600 ℃ (c) T= 1000 ℃

Based on the data obtained, the amount of doping used can affect the Reflection Coefficient (RC) value in the sample. The RC value and absorption coefficient greatly affect the absorption power of microwaves produced by the sample. If the reflection coefficient value is smaller, the resulting wave reflection will also be less, or, in other words, it can minimize wave reflection [64,65]. The requirements that must be met in making microwave absorbing materials are that the materials used must have a high conductivity value because they are good for use as absorbing materials [63,66].

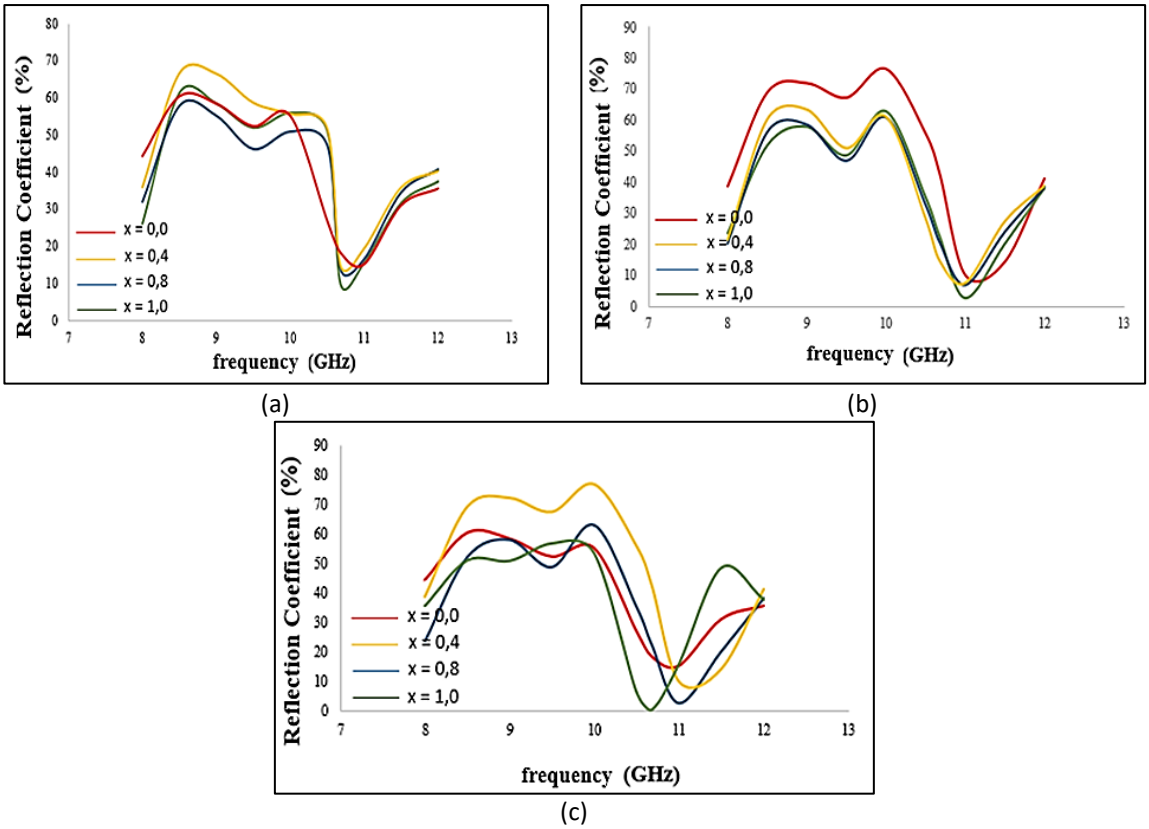

Fig. 7. Value chart RC (%) at x = 0.0, 0.4, 0.8, and 1.0 with (a) T= 200 ℃ (b) T= 600 ℃; (c) T= 1000 ℃

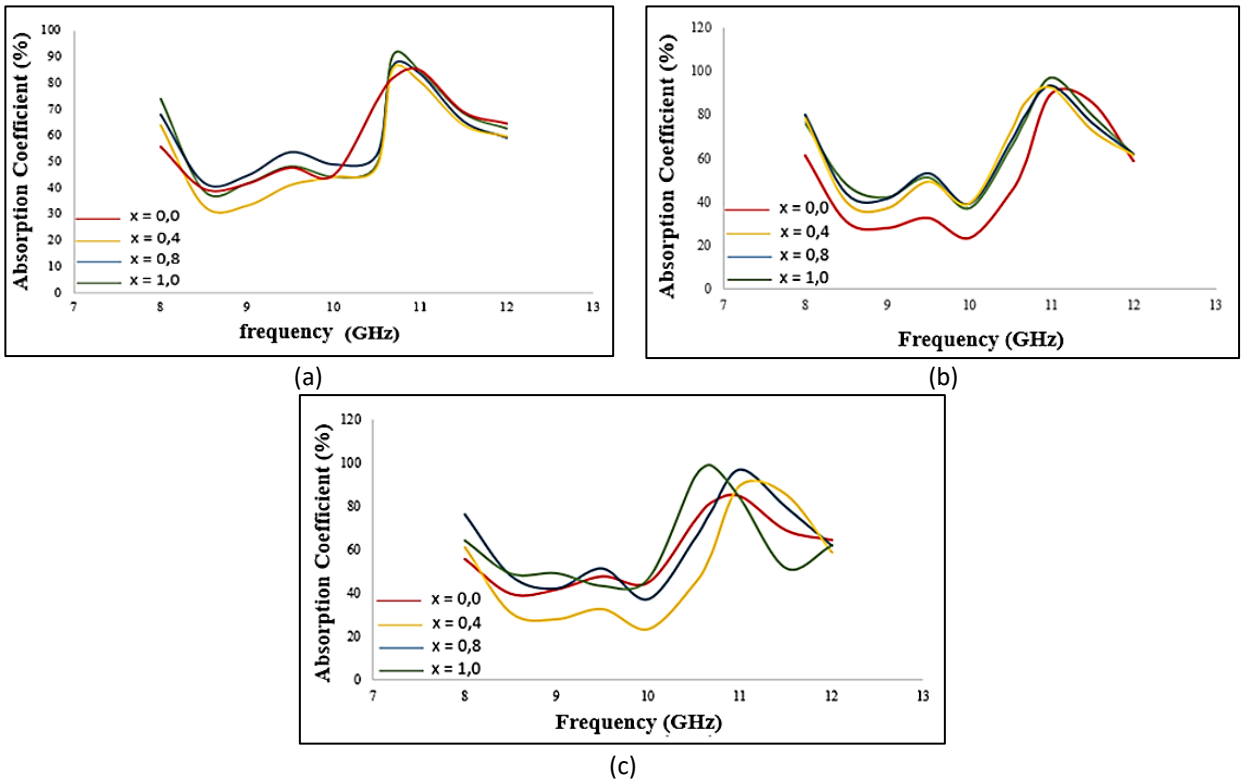

Fig. 8. Value chart A (%) at x = 0.0, 0.4, 0.8, and 1.0 with (a) T= 200 ℃ (b) T= 600 ℃ (c) T= 1000 ℃

Figure 8 shows that the absorption value is 99.31% in the range of 10.68 GHz, so that the sample (mole fraction (x)=1.0) can be used as a microwave-absorbing material with a high absorption

capacity. Based on the results of the data obtained, the amount of doping used can affect the RL value in the sample. The value of RL and the absorption coefficient greatly affect the absorption of microwaves produced by the sample. The greater the value of RL (dB) produced, the higher the percentage of absorption. The condition that must be met in making microwave absorbing materials is that the materials used must have a high conductivity value, because they are good for use as absorbent materials.

4. Conclusions

Based on the results and discussion above, it can be concluded that BaM ($BaFe_{12}O_{19}$) based on natural iron sand with Cobalt-Cupper-Zink metal ion doping produces peaks at certain wave numbers according to the wave number characterization of each peak, namely Ba-O (1.124 cm^{-1}), Fe-O (542 cm^{-1}), Co-O, Cu-O and Zn-O (469 cm^{-1}). The particle sizes in the sample are included in nanoparticles, which are 50 nm in size, and there are components that have been formed, namely hexagonal. For the properties of the RAM material, namely the magnetic properties of the material, the Hc value decreases with the Ms and Mr values increasing at each concentration at each temperature. This shows that the sample is soft magnetic and in accordance with the theory. In addition to the magnetic properties of the material, the sample is also included in the semiconductor material, where the best sample is obtained at (mole fraction (x) = 1.0) with a temperature of T = 1000 ℃ because it has a conductivity value ranging from 10^{-3} S/ cm up to 10^{-1} S/cm with the highest RL value obtained, which is -21.64 dB which produces an absorption value of 99.31%, so that the sample (mole fraction (x) = 1.0) with a temperature of T = 1000 ℃ can be used as a microwave absorbent material with high absorption ability.

Acknowledgement

The author would like to thank all parties who have helped in this research process, especially the Analytical Laboratory, Basic Chemistry Laboratory, and Advanced Chemistry Laboratory of the Faculty of Mathematics and Natural Sciences, University of Mataram, Metallurgy Laboratory, Nanoscience and Nanotechnology Laboratory, Bandung Institute of Technology, and Integrated Research and Testing Laboratory, Gadjah Mada University.

References

[1] Shukla, Vineeta. "Review of electromagnetic interference shielding materials fabricated by iron ingredients." *Nanoscale Advances* 1, no. 5 (2019): 1640-1671. https://doi.org/10.1039/C9NA00108E

[2] Vinnik, Denis A., Aleksandra Yu Tarasova, Dmitry A. Zherebtsov, Svetlana A. Gudkova, Damir M. Galimov, Vladimir E. Zhivulin, Evgeny A. Trofimov, Sandra Nemrava, Nikolai S. Perov, Ludmila I. Isaenko, and Rainer Niewa. "Magnetic and structural properties of barium hexaferrite BaFe12O19 from various growth techniques." *Materials* 10, no. 6 (2017): 578. https://doi.org/10.3390/ma10060578

[3] Jian, Xian, Biao Wu, Yufeng Wei, Shi Xue Dou, Xiaolin Wang, Weidong He, and Nasir Mahmood. "Facile synthesis of Fe3O4/GCs composites and their enhanced microwave absorption properties." *ACS Applied Materials & Interfaces* 8, no. 9 (2016): 6101-6109. https://doi.org/10.1021/acsami.6b00388

[4] Afghahi, Seyyed Salman Seyyed, Mojtaba Jafarian, Mohsen Salehi, and Yomen Atassi. "Improvement of the performance of microwave X band absorbers based on pure and doped Ba-hexaferrite." *Journal of Magnetism and Magnetic Materials* 421 (2017): 340-348. https://doi.org/10.1016/j.jmmm.2016.08.042

[5] Pullar, Robert C. "Hexagonal ferrites: a review of the synthesis, properties and applications of hexaferrite ceramics." *Progress in Materials Science* 57, no. 7 (2012): 1191-1334. https://doi.org/10.1016/j.pmatsci.2012.04.001

[6] Zhao, Tingkai, Wenbo Jin, Yixue Wang, Xianglin Ji, Huibo Yan, Chuanyin Xiong, Xufei Lou, Alei Dang, Hao Li, and Tiehu Li. "In situ synthesis and electromagnetic wave absorbing properties of sandwich microstructured graphene/La-doped barium ferrite nanocomposite." *RSC Advances* 7, no. 59 (2017): 37276-37285. https://doi.org/10.1039/C7RA06716J

[7] Wang, Hefei, Yuanguo Xu, Liquang Jing, Shuquan Huang, Yan Zhao, Minqiang He, Hui Xu, and Huaming Li. "Novel magnetic BaFe12O19/g-C3N4 composites with enhanced thermocatalytic and photo-Fenton activity under visible-light." *Journal of Alloys and Compounds* 710 (2017): 510-518. https://doi.org/10.1016/j.jallcom.2017.03.144

[8] Gultom, Golfrid, Martha Rianna, Perdamean Sebayang, and Masno Ginting. "The effect of Mg–Al binary doped barium hexaferrite for enhanced microwave absorption performance." *Case Studies in Thermal Engineering* 18 (2020): 100580. https://doi.org/10.1016/j.csite.2019.100580

[9] Guler, Emine, Hakan Can Soyleyici, Dilek Odaci Demirkol, Metin Ak, and Suna Timur. "A novel functional conducting polymer as an immobilization platform." *Materials Science and Engineering: C* 40 (2014): 148-156. https://doi.org/10.1016/j.msec.2014.03.063

[10] Qindeel, Rabia, Norah H. Alonizan, Eman A. Alghamdi, and Manal A. Awad. "Synthesis and characterization of spinel ferrites for microwave devices." *Journal of Sol-Gel Science and Technology* 97 (2021): 593-599. https://doi.org/10.1007/s10971-021-05470-9

[11] Yu, Sheng-Hui, Qian-Lin Wang, Yao Chen, Yan Wang, and Jia-Hong Wang. "Microwave-assisted synthesis of spinel ferrite nanospherolites." *Materials Letters* 278 (2020): 128431. https://doi.org/10.1016/j.matlet.2020.128431

[12] Xie, JianLiang, Mangui Han, Liang Chen, Renxiong Kuang, and Longjiang Deng. "Microwave-absorbing properties of NiCoZn spinel ferrites." *Journal of Magnetism and Magnetic Materials* 314, no. 1 (2007): 37-42. https://doi.org/10.1016/j.jmmm.2007.02.124

[13] Teber, Ahmet, Kadir Cil, Turgut Yilmaz, Busra Eraslan, Dilara Uysal, Gokce Surucu, Abdul H. Baykal, and Rajeev Bansal. "Manganese and zinc spinel ferrites blended with multi-walled carbon nanotubes as microwave absorbing materials." *Aerospace* 4, no. 1 (2017): 2. https://doi.org/10.3390/aerospace4010002

[14] Awadallah, Ahmad, Sami H. Mahmood, Yazan Maswadeh, Ibrahim Bsoul, Mufeed Awawdeh, Qassem I. Mohaidat, and Hassan Juwhari. "Structural, magnetic, and Mössbauer spectroscopy of Cu substituted M-type hexaferrites." *Materials Research Bulletin* 74 (2016): 192-201. https://doi.org/10.1016/j.materresbull.2015.10.034

[15] Shao, Li-Huan, Si-Yun Shen, Hui Zheng, Peng Zheng, Qiong Wu, and Liang Zheng. "Effect of powder grain size on microstructure and magnetic properties of hexagonal barium ferrite ceramic." *Journal of Electronic Materials* 47 (2018): 4085-4089. https://doi.org/10.1007/s11664-018-6301-y

[16] Lin, Ying, Yiran Liu, Jingjing Dai, Lei Wang, and Haibo Yang. "Synthesis and microwave absorption properties of plate-like $BaFe_{12}O_{19}$@ Fe_3O_4 core-shell composite." *Journal of Alloys and Compounds* 739 (2018): 202-210. https://doi.org/10.1016/j.jallcom.2017.12.086

[17] Kanagesan, S., S. Jesurani, M. Sivakumar, C. Thirupathi, and T. Kalaivani. "Effect of Microwave Calcinations on Barium Hexaferrite Synthesized via Sol-Gel Combustion." *Journal of Scientific Research* 3, no. 3 (2011). https://doi.org/10.3329/jsr.v3i3.6483

[18] Primc, Darinka, Darko Makovec, Darja Lisjak, and Mihael Drofenik. "Hydrothermal synthesis of ultrafine barium hexaferrite nanoparticles and the preparation of their stable suspensions." *Nanotechnology* 20, no. 31 (2009): 315605. https://doi.org/10.1088/0957-4484/20/31/315605

[19] Anand, S., S. Pauline, and C. Joseph Prabagar. "Zr doped Barium hexaferrite nanoplatelets and RGO fillers embedded Polyvinylidenefluoride composite films for electromagnetic interference shielding applications." *Polymer Testing* 86 (2020): 106504. https://doi.org/10.1016/j.polymertesting.2020.106504

[20] Bañuelos-Frías, Alan, Gerardo Martínez-Guajardo, Leo Alvarado-Perea, Lázaro Canizalez-Dávalos, Facundo Ruiz, and Claudia Valero-Luna. "Light absorption properties of mesoporous barium hexaferrite, $BaFe_{12}O_{19}$." *Materials Letters* 252 (2019): 239-243. https://doi.org/10.1016/j.matlet.2019.05.137

[21] Chen, Min, Run Hua Fan, Zi Dong Zhang, Yan Sheng Yin, and Li Hua Dong. "Synthesis of Uniform Barium Ferrite Powders by Co-Precipitation Method." In *Materials Science Forum,* 898, p. 1649-1654. Trans Tech Publications Ltd, 2017. https://doi.org/10.4028/www.scientific.net/MSF.898.1649

[22] Rusianto, Toto, M. Waziz Wildan, and Kamsul Abraha. "Characterizations of ceramic magnets from iron sand." *International Journal of Technology* 6, no. 6 (2015). https://doi.org/10.14716/ijtech.v6i6.1572

[23] Harris, Vincent G., Anton Geiler, Yajie Chen, Soack Dae Yoon, Mingzhong Wu, Aria Yang, Zhaohui Chen, Peng He, Patanjali V. Parimi, Xu Zuo, Carl E. Patton, Manasori Abe , Olivier Acher, and Carmine Vittoria. "Recent advances in processing and applications of microwave ferrites." *Journal of Magnetism and Magnetic Materials* 321, no. 14 (2009): 2035-2047. https://doi.org/10.1016/j.jmmm.2009.01.004

[24] Soman, Vaishali V., V. M. Nanoti, and D. K. Kulkarni. "Dielectric and magnetic properties of Mg–Ti substituted barium hexaferrite." *Ceramics International* 39, no. 5 (2013): 5713-5723. https://doi.org/10.1016/j.ceramint.2012.12.089

[25] Sonal, Singhal, Kaur Kirandish, Jauhar Sheenu, and Bhukal Santosh. "Structural and magnetic properties of BaCo x Fe 12x O 19 (x= 0.2, 0.4, 0.6, &1. 0) nanoferrites synthesized via citrate sol-gel method." *World Journal of Condensed Matter Physics* 2011 (2011). https://doi.org/10.4236/wjcmp.2011.13016

[26] Sari, Ayu Yuswita, Cut Hani Safira, Eko Arief Setiadi, Silviana Simbolon, Candra Kurniawan, and Perdamean Sebayang. "Efek aditif FeMo dan proses kalsinasi pada serbuk magnetik $BaFe_{12}O_{19}$." *Jurnal Sains Materi Indonesia* 18, no. 3 (2018): 95-100. https://doi.org/10.17146/jsmi.2017.18.3.4112

[27] Rianna, Martha, Marhaposan Situmorang, Candra Kurniawan, Anggito P. Tetuko, Eko Arief Setiadi, Masno Ginting, and Perdamean Sebayang. "The effect of Mg-Al additive composition on microstructure, magnetic properties, and microwave absorption on BaFe12− 2xMgxAlxO19 (x= 0–0.5) material synthesized from natural iron sand." *Materials Letters* 256 (2019): 126612. https://doi.org/10.1016/j.matlet.2019.126612

[28] Ghzaiel, Tayssir Ben, Wadia Dhaoui, Frédéric Schoenstein, Philippe Talbot, and Frédéric Mazaleyrat. "Substitution effect of Me= Al, Bi, Cr and Mn to the microwave properties of polyaniline/BaMeFe11O19 for absorbing electromagnetic waves." *Journal of Alloys and Compounds* 692 (2017): 774-786. https://doi.org/10.1016/j.jallcom.2016.09.075

[29] Wu, K. H., T. H. Ting, G. P. Wang, C. C. Yang, and C. W. Tsai. "Synthesis and microwave electromagnetic characteristics of bamboo charcoal/polyaniline composites in 2–40 GHz." *Synthetic Metals* 158, no. 17-18 (2008): 688-694. https://doi.org/10.1016/j.synthmet.2008.04.013

[30] Ansari, Fatemeh, Faezeh Soofivand, and Masoud Salavati-Niasari. "Eco-friendly synthesis of cobalt hexaferrite and improvement of photocatalytic activity by preparation of carbonic-based nanocomposites for waste-water treatment." *Composites Part B: Engineering* 165 (2019): 500-509. https://doi.org/10.1016/j.compositesb.2019.02.010

[31] Mallick, Kajal K., Philip Shepherd, and Roger J. Green. "Magnetic properties of cobalt substituted M-type barium hexaferrite prepared by co-precipitation." *Journal of Magnetism and Magnetic Materials* 312, no. 2 (2007): 418-429. https://doi.org/10.1016/j.jmmm.2006.11.130

[32] Kumar, Narenda, and Rajiv Kumar. *Nanotechnology and Nanomaterials in the Treatment of Life-threatening Diseases: Nanomedicine, diagnostics and drug delivery*. William Andrew, 2013.

[33] Wei, Guoke, Tao Wang, Hang Zhang, Xiaotong Liu, Yinlong Han, Yanchun Chang, Liang Qiao, and Fashen Li. "Enhanced microwave absorption of barium cobalt hexaferrite composite with improved bandwidth via c-plane alignment." *Journal of Magnetism and Magnetic Materials* 471 (2019): 267-273. https://doi.org/10.1016/j.jmmm.2018.09.063

[34] Doyan, Aris, Ilham Halik, and Susilawati Susilawati. "Pengaruh variasi temperatur kalsinasi terhadap barium m-heksaferit didoping Zn menggunakan Fourier transform infra red." Jurnal Pijar Mipa 10, no. 1 (2015). https://doi.org/10.29303/jpm.v10i1.9

[35] Setiadi, E. A., P. Sebayang, M. Ginting, A. Y. Sari, C. Kurniawan, C. S. Saragih, and P. Simamora. "The synthesization of Fe3O4 magnetic nanoparticles based on natural iron sand by co-precipitation method for the used of the adsorption of Cu and Pb ions." In *Journal of Physics: Conference Series*, 776, no. 1, p. 012020. IOP Publishing, 2016. https://doi.org/10.1088/1742-6596/776/1/012020

[36] Stuart, Barbara H. Infrared spectroscopy: Fundamentals and applications. John Wiley & Sons, 2004. https://doi.org/10.1002/0470011149

[37] Jang, Hyun Tae, Eui Min Jung, Sang Hyun Park, and Pushparaj Hemalatha. "Synthesis and characterization of CoO-ZnO catalyst system for selective CO oxidation." *International Journal of Control and Automation* 8, no. 6 (2013): 31-40. https://doi.org/10.14257/ijca.2013.6.6.04

[38] Priyo, Wahyu. "Manfaat nanopartikel di bidang kesehatan." *Majalah Farmasetika* 2, no. 4 (2017): 1-3. https://doi.org/10.24198/farmasetika.v2i4.15891

[39] Patil-Sen, Yogita, Enza Torino, Franca De Sarno, Alfonso Maria Ponsiglione, Vikesh Chhabria, Waqar Ahmed, and Tim Mercer. "Biocompatible superparamagnetic core-shell nanoparticles for potential use in hyperthermia-enabled drug release and as an enhanced contrast agent." *Nanotechnology* 31, no. 37 (2020): 375102. https://doi.org/10.1088/1361-6528/ab91f6

[40] Dawar, Naini, Mansi Chitkara, Inderjeet Singh Sandhu, Jaspreet Singh Jolly, and Shivani Malhotra. "Structural, magnetic and dielectric properties of pure and nickel-doped barium nanohexaferrites synthesized using chemical co-precipitation technique." *Cogent Physics* 3, no. 1 (2016): 1208450. https://doi.org/10.1080/23311940.2016.1208450

[41] Li, X. X., J. J. Zhou, J. X. Deng, H. Zheng, L. Zheng, P. Zheng, and H. B. Qin. "Synthesis of dense, fine-grained YIG ceramics by two-step sintering." *Journal of Electronic Materials* 45 (2016): 4973-4978. https://doi.org/10.1007/s11664-016-4690-3

[42] Mohammed, Abdur Raheem, Mohiddin shaw Shaik, Mohana Ramana Ravuri, Maheswari Ch, and Dharmaiah Gurram. "Thermophoresis, brownian diffusion, porosity, and magnetic parameters' effects on three-dimensional rotating Ag-CuO/H_2O hybrid nanofluid flow across a linearly stretched sheet with aligned magnetic field." *CFD Letters* 15, no. 10 (2023): 123-151. https://doi.org/10.37934/cfdl.15.10.123151

[43] Jamalian, Majid, Ali Ghasemi, and Ebrahim Paimozd. "Sol–gel synthesis of Mn–Sn–Ti-substituted strontium hexaferrite nanoparticles: structural, magnetic, and reflection-loss properties." *Journal Of Electronic Materials* 43 (2014): 1076-1082. https://doi.org/10.1007/s11664-014-2984-x

[44] Harahap, Veryyon, and Anju Bherna D. Nainggolan. "Coating radiation waves based on $BaFe_{12}O_{19}$/ZnO from natural red sand on X-ray radiation exposure in the Laboratory of Efarina Hospital in the era of the COVID-19 pandemic." *Journal of Aceh Physics Society* 11, no. 1 (2022): 17-23. https://doi.org/10.24815/jacps.v11i1.21871

[45] Doyan, Aris, Susilawati Susilawati, Agus Abhi Purwoko, Muhammad Taufik, Dedi Riyan Rizaldi, and Ziadatul Fatimah. "Synthesis and characterization of cobalt-doped titanium dioxide thin films as solar cell components using UV-SEM analysis." *Journal of Advanced Research in Micro and Nano Engineering* 21, no. 1 (2024): 1-15. https://doi.org/10.37934/armne.21.1.115

[46] Braun, Adelina, Vikram Kestens, Katrin Franks, Gert Roebben, Andrée Lamberty, and Thomas PJ Linsinger. "A new certified reference material for size analysis of nanoparticles." *Journal of Nanoparticle Research* 14 (2012): 1-12. https://doi.org/10.1007/s11051-012-1021-3

[47] Oktavia, Intan Nabilah, and Suyatno Sutoyo. "Review artikel: Sintesis nanopartikel perak menggunakan bioreduktor ekstrak tumbuhan sebagai bahan antioksidan." UNESA Journal of Chemistry 10, no. 1 (2021): 37-54. https://doi.org/10.26740/ujc.v10n1.p37-54

[48] Abram, Sarah-Luise, Paul Mrkwitschka, Andreas F. Thünemann, Jörg Radnik, Ines Häusler, Harald Bresch, Vasile-Dan Hodoroaba, and Ute Resch-Genger. "Iron oxide nanocubes as a new certified reference material for nanoparticle size measurements." *Analytical Chemistry* 95, no. 33 (2023): 12223-12231. https://doi.org/10.1021/acs.analchem.3c00749

[49] Recknagel, Sebastian, Harald Bresch, Heinrich Kipphardt, Matthias Koch, Martin Rosner, and Ute Resch-Genger. "Trends in selected fields of reference material production." *Analytical and Bioanalytical Chemistry* 414, no. 15 (2022): 4281-4289. https://doi.org/10.1007/s00216-022-03996-7

[50] Liu, Jinjie, Xiaohua Feng, Shuangjie Wu, Ping Zhou, Jing Huang, Hua Li, and Tongxiang Liang. "High microwave absorption performance in Nd-substituted BaM/GO through sol-gel and high energy ball milling process." *Journal of Alloys and Compounds* 892 (2022): 162207. https://doi.org/10.1016/j.jallcom.2021.162207

[51] Liu, Chuyang, Yanting Zhang, Haonan Gong, Yunjia Hu, Songhan Duan, Kangsen Peng, and Kongjun Zhu. "Facile fabrication of rGO/Zr4+-Ni2+ gradient-doped BaM composites for broad microwave absorption bandwidth." *Ceramics International* 47, no. 3 (2021): 4333-4337. https://doi.org/10.1016/j.ceramint.2020.09.273

[52] Prabagar, C. Joseph, S. Anand, M. Asisi Janifer, and S. Pauline. "Structural and magnetic properties of Mn doped cobalt ferrite nanoparticles synthesized by Sol-Gel auto combustion method." *Materials Today: Proceedings* 47 (2021): 2013-2019. https://doi.org/10.1016/j.matpr.2021.04.209

[53] Yudhawardana, Hartoyo, and Heri F. Lalus. "Analysis of chemical compound content and magnetic properties of iron sand in Rondo Woing Village, East Manggarai." *Jurnal Pendidikan Fisika dan Teknologi* 9, no. 1 (2023): 133-142. https://doi.org/10.29303/jpft.v9i1.4897

[54] Van Zijl, Peter CM, Wilfred W. Lam, Jiadi Xu, Linda Knutsson, and Greg J. Stanisz. "Magnetization transfer contrast and chemical exchange saturation transfer MRI. Features and analysis of the field-dependent saturation spectrum." *Neuroimage* 168 (2018): 222-241. https://doi.org/10.1016/j.neuroimage.2017.04.045

[55] Hadadian, Yaser, Ana Paula Ramos, and Theo Z. Pavan. "Role of zinc substitution in magnetic hyperthermia properties of magnetite nanoparticles: Interplay between intrinsic properties and dipolar interactions." *Scientific Reports* 9, no. 1 (2019): 18048. https://doi.org/10.1038/s41598-019-54250-7

[56] Yamato, Masafumi, and Tsunehisa Kimura. "Magnetic processing of diamagnetic materials." *Polymers* 12, no. 7 (2020): 1491. https://doi.org/10.3390/polym12071491

[57] Urzhumtsev, Andrey, Viktoria Maltseva, and Aleksey Volegov. "Magnetization reversal processes in sintered permanent magnets Sm (Co, Fe, Zr, Cu) z." *Journal of Magnetism and Magnetic Materials* 551 (2022): 169143. https://doi.org/10.1016/j.jmmm.2022.169143

[58] Algarou, Norah Abdullah, Y. Slimani, Munirah Abdullah Almessiere, A. Baykal, S. Guner, A. Manikandan, and Ismail Ercan. "Enhancement on the exchange coupling behavior of SrCo0. 02Zr0. 02Fe11. 96O19/MFe2O4 (M= Co, Ni, Cu, Mn and Zn) as hard/soft magnetic nanocomposites." *Journal of Magnetism and Magnetic Materials* 499 (2020): 166308. https://doi.org/10.1016/j.jmmm.2019.166308

[59] Ye, Zhantong, Yaqin Qie, Zhipeng Fan, Yixuan Liu, and Hua Yang. "Exchange-coupled of soft and hard magnetic phases on the interfaces of $Fe_3C/CoFe_2O_4$ nanocomposites." *Ceramics International* 46, no. 1 (2020): 731-736. https://doi.org/10.1016/j.ceramint.2019.09.026

[60] Mahmood, Sami H., Aynour N. Aloqaily, Yazan Maswadeh, Ahmad Awadallah, Ibrahim Bsoul, Mufeed Awawdeh, and Hassan Juwhari. "Effects of heat treatment on the phase evolution, structural, and magnetic properties of Mo-Zn doped M-type hexaferrites." *Solid State Phenomena* 232 (2015): 65-92. https://doi.org/10.4028/www.scientific.net/SSP.232.65

[61] Hambali, Susilawati, and Aris Doyan. "Synthesis and characterization barium M-hexaferrites (BaFe12-2xCoxMnxNixO19) as a microwave absorbent material." *Solid State Phenomena* 317 (2021): 46-52. https://doi.org/10.4028/www.scientific.net/SSP.317.46

[62] Mishra, Radha Raman, and Apurbba Kumar Sharma. "Microwave–material interaction phenomena: Heating mechanisms, challenges and opportunities in material processing." *Composites Part A: Applied Science and Manufacturing* 81 (2016): 78-97. https://doi.org/10.1016/j.compositesa.2015.10.035

[63] Elmahaishi, Madiha Fathi, Ismayadi Ismail, and Farah Diana Muhammad. "A review on electromagnetic microwave absorption properties: Their materials and performance." *Journal of Materials Research and Technology* 20 (2022): 2188-2220. https://doi.org/10.1016/j.jmrt.2022.07.140

[64] Gao, Junliang, Xiaozhou Ma, Guohai Dong, Hongzhou Chen, Qian Liu, and Jun Zang. "Investigation on the effects of Bragg reflection on harbor oscillations." *Coastal Engineering* 170 (2021): 103977. https://doi.org/10.1016/j.coastaleng.2021.103977

[65] Mackay, Ed, and Lars Johanning. "Comparison of analytical and numerical solutions for wave interaction with a vertical porous barrier." *Ocean Engineering* 199 (2020): 107032. https://doi.org/10.1016/j.oceaneng.2020.107032

[66] Houbi, Anas, Zharmenov A. Aldashevich, Yomen Atassi, Z. Bagasharova Telmanovna, Mirzalieva Saule, and Kadyrakunov Kubanych. "Microwave absorbing properties of ferrites and their composites: A review." *Journal of Magnetism and Magnetic Materials* 529 (2021): 167839. https://doi.org/10.1016/j.jmmm.2021.167839